

# Effect of Membrane Tension on Gap Junctional Conductance of Supporting Cells in Corti's Organ

HONG-BO ZHAO and J. SANTOS-SACCHI

From the Sections of Otolaryngology and Neurobiology, Yale University School of Medicine, New Haven, Connecticut 06510

**ABSTRACT** The effects of turgor pressure-induced membrane tension on junctional coupling of Hensen cell isolates from the inner ear were evaluated by input capacitance or transjunctional conductance measurement techniques. Turgor pressure was altered by changing either pipette pressure or the osmolarities of extracellular solutions. Both positive pipette pressure and extracellular applications of hypotonic solutions, which caused cell size to concomitantly increase, uncoupled the cells as indicated by reduced input capacitance and transjunctional conductance. These changes were, in many cases, reversible and repeatable. Intracellular application of 50  $\mu$ M H-7, a broad-based protein kinase inhibitor, and 10 mM BAPTA did not block the uncoupling effect of positive turgor pressure on inner ear gap junctions. The transjunctional conductance at a holding potential of  $-80$  mV was  $53.6 \pm 5.8$  nS (mean  $\pm$  SEM,  $n = 9$ ) and decreased  $\sim 40\%$  at a turgor pressure of  $1.41 \pm 0.05$  kPa. Considering the coincident kinetics of cell deformation and uncoupling, we speculate that mechanical forces work directly on gap junctions of the inner ear. These results suggest that pathologies that induce imbalances in cochlear osmotic pressure regulation may compromise normal cochlear homeostasis.

**KEY WORDS:** cochlea • membrane tension • turgor pressure • gap junctions • Hensen cells

## INTRODUCTION

The supporting cells of the organ of Corti are structurally and electrically coupled together by gap junctions (Jahnke, 1975; Gulley and Reese, 1976; Iurato et al., 1976; Hama and Saito, 1977; Santos-Sacchi and Dallos, 1983; Kikuchi et al., 1995). Such gap junctional coupling among the supporting cells provides for electrical and metabolic uniformity; cochlear homeostasis is believed to rely on intercellular coupling (Santos-Sacchi, 1985, 1986, 1991; Kikuchi et al., 1995).

Gap junction channels are distinguished from other ionic channels since the integration of two aligned hemichannels from adjacent cells is required for normal function. In early work, hypertonic solutions, which cause cell and tissue shrinkage, were found to uncouple gap junctions in several different preparations (Barr et al., 1965, 1968; Goodenough and Gilula, 1974; Loewenstein et al., 1967). More recently, hypotonic treatments, which cause cell swelling, were determined to either increase (Kimelberg and Kettenmann, 1990) or decrease (Ngezahayo and Kolb, 1990) gap junctional coupling. These effects could have been due

to a variety of factors, including direct mechanical influences, changes in nonjunctional resistance, and modulation of intracellular factors that are known to uncouple cells. In the study of Ngezahayo and Kolb (1990), where junctional conductance was studied directly, the decrease in coupling was abolished by 5 mM EGTA in nominally  $\text{Ca}^{2+}$ -free internal solutions, and was linked to the activity of PKC. In the present report, we used the whole-cell voltage clamp technique to examine the effects of turgor pressure on junctional coupling of isolated pairs or small groups of cochlear supporting cells. Both input capacitance (Santos-Sacchi, 1991; Bigiani and Roper, 1995) and transjunctional conductance measures were used to gauge intercellular communication. We report that data obtained with both techniques indicate that positive intracellular pressure, which is known to induce membrane tension, uncouples gap junctions of supporting cells in Corti's organ.

## METHODS

Detailed experimental methods can be found in previous reports (Santos-Sacchi, 1991; Sato and Santos-Sacchi, 1994). In brief, isolated supporting cells or cell aggregates were freshly obtained from the organ of Corti of the guinea pig cochlea by shaking for 5–15 min in nominally  $\text{Ca}^{2+}$ -free Leibovitz medium containing 1 mg/ml trypsin. To reduce the voltage-dependent ionic currents from nonjunctional membrane during double voltage clamp experiments, cells were perfused with an ionic blocking solution containing (mM): 100 NaCl, 20 TEA, 20 CsCl, 1.25  $\text{CoCl}_2$ , 1.48  $\text{MgCl}_2$ , 10 HEPES, pH 7.2, 300 mosM. In initial experiments, a modified Leibovitz medium was used for measurement of input

---

Portions of this work were previously published in abstract form (Zhao, H.B., and J. Santos-Sacchi. 1997. *Assoc. Res. Otolaryngol.* St. Petersburg, FL, pp. 15).

Address correspondence to Joseph Santos-Sacchi, Ph.D., Professor, Surgery (Otolaryngology), BML 244, Yale University School of Medicine, 333 Cedar St., New Haven, CT 06510. Fax: 203-737-2245; E-mail: joseph.santos-sacchi@yale.edu

capacitance ( $C_{in}$ )<sup>1</sup> with a single pipette voltage clamp containing (mM): 136.9 NaCl, 5.37 KCl, 1.25 CaCl<sub>2</sub>, 1.48 MgCl<sub>2</sub>, 10 HEPES, pH 7.2, 300 mosM. Pipette solutions were composed of (mM): 140 KCl, 10 EGTA or BAPTA, 2 MgCl<sub>2</sub>, and 10 HEPES, pH 7.2. For double voltage clamp recording, 140 mM KCl was replaced with 140 mM CsCl. Patch electrodes had initial resistances of 2.5–4 MΩ, corresponding to 1–2 μm in diameter. Series resistance ( $R_s$ ) after whole cell configuration was estimated from the current in response to 10-mV steps (Huang and Santos-Sacchi, 1993). In single Hensen cells, where  $R_s$  could be unequivocally determined after whole cell configuration, the average value was  $7.16 \pm 0.43$  MΩ (mean  $\pm$  SEM,  $n = 48$ ). Cells were typically held at  $-80$  mV, within the Hensen cell's linear current-voltage range (Santos-Sacchi, 1991). Currents were filtered at 10 kHz with a four-pole Bessel filter (Axon Instruments, Foster City, CA). Intracellular pressure was modified either through the patch pipette with a syringe connected to the Teflon<sup>®</sup> tubing attached to the patch pipette holder or by changing osmolarity with "Y-tube" bath perfusion. Pipette pressure was monitored via a T-connector to a pressure monitor (World Precision Instruments, Inc., Sarasota, FL). All experiments were video tape recorded and performed at room temperature.

Since the input capacitance can be measured by a single pipette voltage clamp and is correlated with junctional conductance (Santos-Sacchi, 1991; Bigiani and Roper, 1995), it can be conveniently used to study gap junctional coupling under conditions of less cellular damage than the double voltage clamp technique. Input capacitance, in conjunction with input resistance ( $R_{in}$ ), was continually measured on line to monitor junctional coupling.  $C_{in}$  and  $R_{in}$  were determined from the transient charge and steady state current, respectively, induced by small ( $-10$  mV) test pulses with duration of  $18\times$  the clamp time constant at the holding potential; measures were made at  $\sim 1$ – $3$  Hz (Santos-Sacchi, 1991).

$$C_{in} = \frac{Q_{in}}{V_{test}} \quad (1)$$

$$R_{in} = \frac{V_{test}}{\Delta I_{\infty}} \quad (2)$$

where

$$Q_{in} = \int_0^{\infty} I_c dt \quad (3)$$

$Q_{in}$  is the charge moved,  $V_{test}$  is the voltage of the test pulse,  $I_c$  is the capacitive current induced by the test pulse, and  $\Delta I_{\infty}$  is the current difference between the steady state current induced by the test pulse and the holding current at the holding potential.

For the double voltage clamp, each cell in a cell pair was separately voltage clamped using 200A and 200B patch clamps (Axon Instruments). Both cells were clamped at the same holding potentials and a test pulse (10 mV, 10 ms) superimposed only on cell 1. The transjunctional current ( $I_j$ ) is equal to the current difference ( $\Delta I_2$ ) in cell 2 caused by the test pulses applied to cell 1. The transjunctional conductance ( $G_j$ ) can be calculated by:

$$G_j = \frac{-\Delta I_2}{V_{test}} \quad (4)$$

where  $V_{test}$  is the test pulse voltage applied to cell 1. Data collection and analysis were performed with an in-house developed

windows-based whole-cell voltage clamp program, jClamp (<http://www.med.yale.edu/surgery/otolar/santos/jclamp.html>), using a Digidata 1200 board (Axon Instruments). In some experiments,  $G_j$  was measured online at 2–4 Hz and the corresponding video images of recorded cells were digitally captured every 5–10 s under software (jClamp) control. The captured images were printed at  $\sim 1,700\times$  and the plane cell areas calculated. To gauge membrane stress, area strain ( $\Delta A/A_0$ ) was calculated, where  $\Delta A$  is the change of cell area after pressure or osmotic treatment and  $A_0$  is the original cell area.

## RESULTS

Hensen cells can be easily distinguished from other inner ear supporting cells by their prominent lipid vacuoles. The number of cells comprising isolates of Hensen cells can be determined under the light microscope, and corresponds to the isolate's  $C_{in}$  since Hensen cells are well coupled electrically. Although the size of Hensen cells is variable, the distributions of  $C_{in}$  for one, two, and three Hensen cells, whose numbers were visually confirmed, were quite distinct (Fig. 1 A). At the

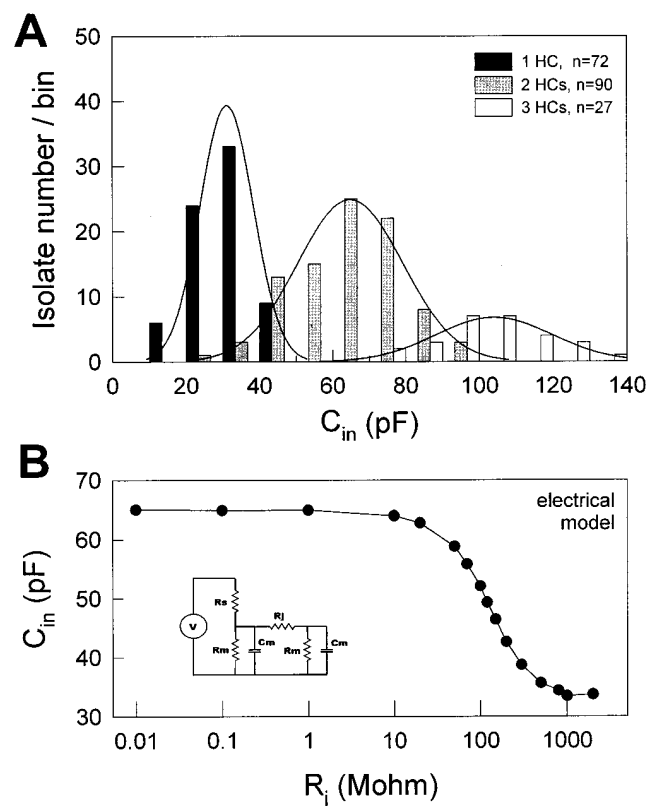


FIGURE 1. (A) The distributions of  $C_{in}$  of Hensen cell (HC) isolates. The cell numbers (1, 2, or 3) in the isolates were determined under the light microscope, and the  $C_{in}$  was obtained at the holding potential  $-80$  mV. Each bar represents the number of isolates within a bin width of 10 pF. The lines plotted over each histogram represent the fitted Gaussian distribution for the three isolate groups. (B)  $C_{in}$  was measured for a coupled two-cell electrical model as transjunctional resistance ( $R_j$ ) was changed.  $R_s$ , 4.7 MΩ;  $R_m$ , 500 MΩ;  $C_m$ , 33 pF. (inset) Coupled two-cell electrical model.

<sup>1</sup>Abbreviations used in this paper:  $C_{in}$ , input capacitance;  $G_j$ , transjunctional conductance; OHC, outer hair cell;  $R_{in}$ , input resistance;  $R_s$ , series resistance.

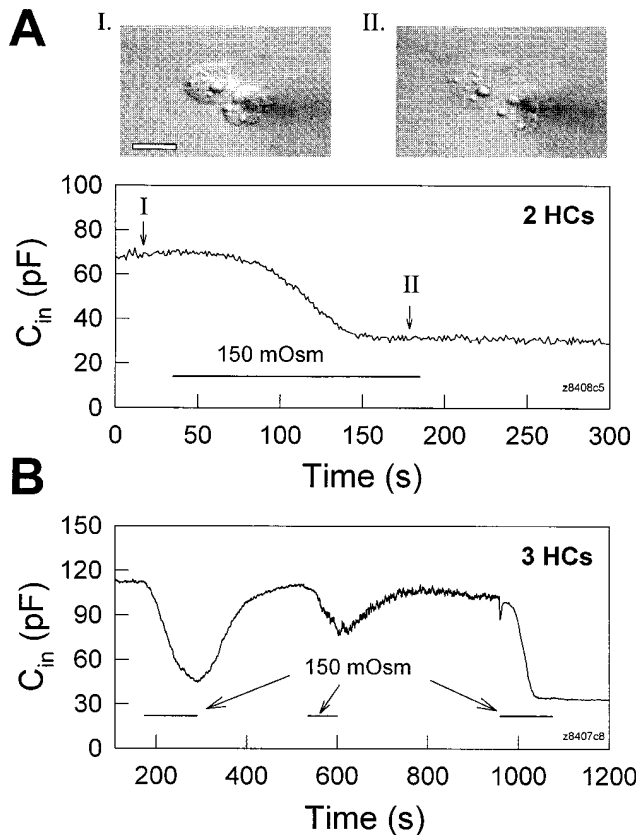


FIGURE 2. Osmolarity-induced turgor pressure increase uncouples Hensen cells. Both bath solution and electrode solution were 300 mosM. (A) When an extracellular 150 mosM solution was perfused (indicated by the horizontal bar) the cell pair swelled (see insets). Concomitantly,  $C_{in}$  decreased to half value due to cell uncoupling.  $R_s$ , 6.5 M $\Omega$ . (insets) Captured cell images before and during the perfusion of the hypo-osmotic solution. The white scale bar represents 20  $\mu$ m. (B) Decreases of  $C_{in}$  due to hypo-osmotic challenge were reversible and repeatable. In this case, the cells finally fully uncoupled and  $C_{in}$  remained at the single cell capacitance level.  $R_s$ , 3.8 M $\Omega$ .

holding potential of  $-80$  mV, the peaks of the isolate distributions were clearly separated at  $31.03 \pm 0.86$ ,  $64.75 \pm 1.5$ , and  $103.9 \pm 3.05$  pF, corresponding to one, two, and three cell contributions, respectively. The number of cells within isolates can also be confirmed using uncoupling agents, such as  $\text{CO}_2$ , octanol, or, as we now find, positive turgor pressure, to uncouple the cells. When cells fully uncoupled,  $C_{in}$  reached single cell capacitance levels (e.g., Figs. 2 and 3). The correlation of  $C_{in}$  with degree of cell coupling is illustrated by real measures of  $C_{in}$  in a coupled two-cell electrical model (Fig. 1 B).  $C_{in}$  of the electrical model was a monotonic function of transjunctional resistance or conductance, indicating the validity of  $C_{in}$  as an indicator of cell coupling.

Positive turgor pressure induced either by osmolarity changes or directly via the patch pipette decreased  $C_{in}$

of cell pairs or three-cell groups (Figs. 2 and 3), but did not reduce single cell capacitance (Fig. 4). This indicates that positive turgor pressure uncouples gap junctions between adjacent Hensen cells.

In Fig. 2 A, bath application of hypo-osmotic solution (150 mosM) caused a Hensen cell pair to swell (insets) and decreased  $C_{in}$  of the pair to single cell levels. The uncoupling induced by increased turgor pressure is reversible since return to normal osmolarity solution often restored initial  $C_{in}$  values; subsequent reperfusion with hypo-osmotic solution remained effective as an uncoupling stimulus (Fig. 2 B). In single cells, while the same hypo-osmotic treatment caused cell swelling,  $C_{in}$  remained stable (Fig. 4 B).

Fig. 3 illustrates the uncoupling effect of cell turgor pressure change induced by patch pipette pressure. As turgor pressure was directly increased to  $\sim 1.2$  kPa via the patch pipette,  $C_{in}$  decreased to almost single cell levels (after an initial delay possibly due to pipette plugging), and immediately began to return when the pressure was released (Fig. 3 A). The cells could be permanently uncoupled during the application of prolonged, continuous positive pressure (Fig. 3 B). The uncoupling effect of positive turgor pressure was found in 40 of 42 cell pairs, or three-cell groups. As with osmolarity change, direct application of positive turgor pressure via the patch pipette also did not decrease the measured capacitance in single Hensen cells despite cell swelling (Fig. 4 A, insets).

Although  $C_{in}$  can be easily measured by single pipette voltage clamp to gauge the degree of cell coupling, transjunctional conductance cannot be measured directly since transjunctional voltage and current are unknown. Additionally, a quantitative estimate of degree of coupling based on  $C_{in}$  is not easily established since  $C_{in}$  is a nonlinear function of transjunctional conductance (see Fig. 1 B and DISCUSSION). To further investigate the uncoupling effect of positive turgor pressure on gap junctions in Hensen cells, the transjunctional conductance was directly assessed with a double voltage clamp technique, and corresponding changes of the cell plane surface areas ( $\Delta A/A_0$ ) (i.e., an indicator of membrane strain) were simultaneously measured.

Figs. 5 and 6 illustrate the results of such experiments. Cell areas increased in concert with decreases of transjunctional conductance as positive turgor pressure was delivered to the cells. The changes in cell area were observable before gap junctional uncoupling and occurred faster than  $G_j$  decay (Figs. 5 and 6). However, unlike pressure changes induced by pipette pressure, hypo-osmotic shocks produced changes in  $G_j$  and cell areas that were quite fast. With extracellular perfusion of a 150-mosM solution, the time constant for  $G_j$  decay was 9.53 s in Fig. 6 B, and the average value was  $5.1 \pm 1.86$  s ( $n = 6$ ). In Fig. 6 B, the rise time constant of

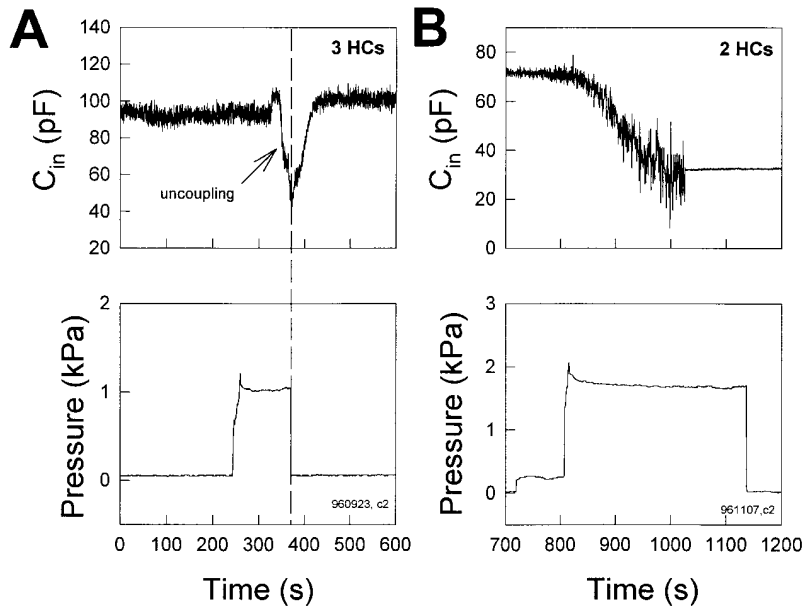


FIGURE 3. Hensen cells uncouple as turgor pressure is directly increased via the patch pipette. (A) In this example, increased pipette pressure caused  $C_{in}$  to decrease to single cell levels after an initial delay (possibly due to pipette plugging), but returned to the original level soon after pipette pressure was released.  $R_s$ , 9.76 M $\Omega$ . (B) A Hensen cell pair uncoupled after prolonged application of pressure.  $C_{in}$  decreased from 71.2 pF to a single cell level of 34.7 pF.  $R_s$ , 8.5 M $\Omega$ .

membrane strain was 4.43 s. The average rise time constant of membrane strain is estimated to be close to or less than that of the average  $G_j$  decay since in most cases the swelling fully occurred within the 5–10-s video capture rate. In most, but not all, cases, it was noted that after membrane tension stabilized, transjunctional conductance likewise stabilized (Fig. 5). The correlated and reciprocal changes in  $G_j$  and membrane strain

( $\Delta A/A_0$ ) were reversible and repeatable (Fig. 6 A), strongly indicating that  $G_j$  decreases were relative to increases of membrane strain; i.e., membrane tension. It should be noted that the latency to  $G_j$  change after  $\Delta A/A_0$  change is possibly due to the absence of significant membrane stress during the initial cell inflation, which clearly (based on the magnitude of cell enlargement) was accompanied by membrane unfolding.

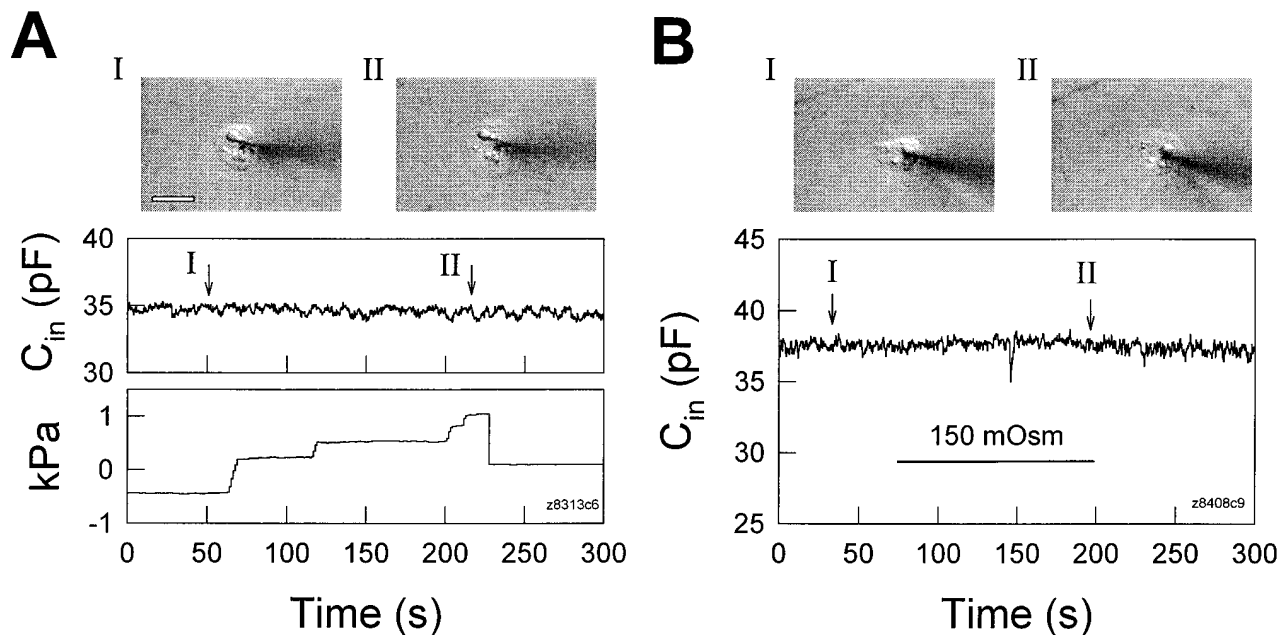


FIGURE 4. Changes of turgor pressure caused either directly via the patch pipette (A) or by perfusion of hypo-osmotic solutions (B) do not decrease the measured capacitance in a single Hensen cell. (insets) Captured cell images before and during applications of positive intracellular pressure. Cell swelling was visible as turgor pressure increased. The white scale bar represents 20  $\mu$ m.  $R_s$ : (A) 8.4 M $\Omega$ , (B) 4.4 M $\Omega$ .

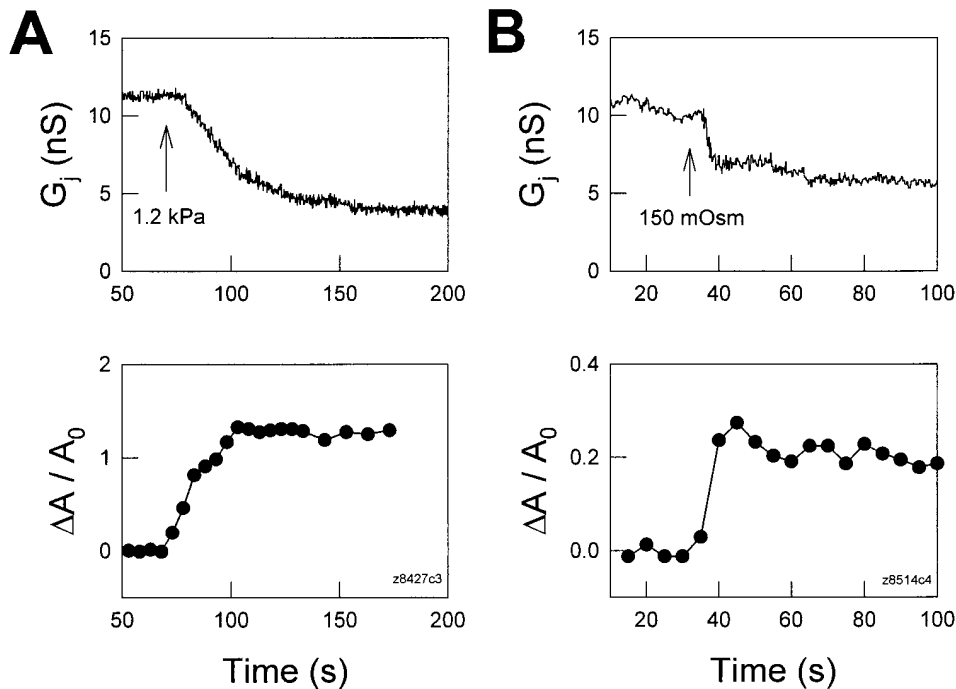


FIGURE 5. Positive turgor pressure-induced reduction in transjunctional conductance is correlated with increases in membrane strain ( $\Delta A/A_0$ ). Transjunctional conductance was measured with a double voltage clamp technique, and membrane strains were calculated from captured images (see METHODS). Each cell in a Hensen cell pair was separately held at  $-40$  mV. The continuous treatments used to increase intracellular pressure began at the arrows. (A) Positive pipette pressure induced an increase in membrane strain and concomitantly reduced  $G_j$ . (B) Perfusion of 150 mosM solution also induced an increase in membrane strain and concomitantly reduced  $G_j$ . The pipette solution contained  $50 \mu\text{M}$  H-7.

Uncoupling of Hensen cell gap junctions by membrane stress was not inhibited by using pipette solutions containing  $50 \mu\text{M}$  H-7 (dihydrochloride; Calbiochem Corp., La Jolla, CA), a broad-based serine/threonine kinase inhibitor (Boulis and Davis, 1990) (Figs. 5 B and 6 B). These data imply that the uncoupling effect of positive turgor pressure on inner ear gap junctions is independent of protein kinases, and that the effect is different from previous observations that cell volume changes induced uncoupling of gap junctions via the PKC pathway (Ngezahayo and Kolb, 1990). Nevertheless, cell swelling induced by hypo-osmotic shocks has been linked to increases of another uncoupling agent, intracellular  $\text{Ca}^{2+}$  (Hoffmann and Simonsen, 1989; Suzuki et al., 1990). However, uncoupling by  $\text{Ca}^{2+}$ , which occurs at millimolar intracellular concentrations in Hensen cells (Sato and Santos-Sacchi, 1994), can be ruled out since pipette solutions contained  $10 \text{ mM}$  BAPTA, a fast highly selective calcium chelating reagent, and extracellular and intracellular solutions were nominally  $\text{Ca}^{2+}$  free. Considering all evidence, the observed uncoupling effect of positive turgor pressure on inner ear gap junctions, which is fast (within seconds), correlated with changes of membrane strain, and independent of protein kinases and  $\text{Ca}^{2+}$ , is likely to occur via direct mechanical effects on the plasmalemma; i.e., membrane tension.

The effect of membrane tension on gap junctional conductance was further studied by increasing turgor pressure in cell 1 and measuring  $I_j$  in cell 2 at different membrane potentials (Fig. 7). Gap junctional conduc-

tance in Hensen cells at a holding potential of  $-80$  mV was  $52.9 \pm 12.1 \text{ nS}$  ( $n = 51$ ). As the turgor pressure in cell 1 was increased,  $I_j$  decreased (Fig. 7 A). The junctional conductance at different membrane potentials reduced in parallel when the turgor pressure was increased. In those cell pairs where turgor pressure alterations were successfully applied without losing the cells,  $G_j$  at  $-80$  mV holding potential decreased  $38.3 \pm 9.5\%$  from  $50.5 \pm 14 \text{ nS}$  ( $n = 9$ ) at a turgor pressure of  $1.41 \pm 0.05 \text{ kPa}$ . The  $V_m$  dependence of  $G_j$  is also visible in Fig. 7. In this case, as the cells were depolarized,  $G_j$  decreased (Fig. 7 B). Other  $V_m$  dependencies of transjunctional conductance were also found, including  $V_m$  insensitivity and an increase with depolarization. Pressure did not alter voltage-dependent behaviors.

#### DISCUSSION

We provide evidence, based on input capacitance and double voltage clamp measures, that junctional coupling is sensitive to positive turgor pressure-induced membrane tension. Turgor pressure has been used to induce membrane tension in a wide variety of cells, including the outer hair cell (OHC), where it has been shown that motility and motility-related gating current characteristics are directly altered (Iwasa, 1993; Gale and Ashmore, 1994; Takehata and Santos-Sacchi, 1995). Membrane tension (possibly acting via cytoskeletal interactions) is also known to gate stretch-activated ionic channels (Yang and Sachs, 1989), which have been observed in outer hair cells (Ding et al., 1991; Iwasa et al.,

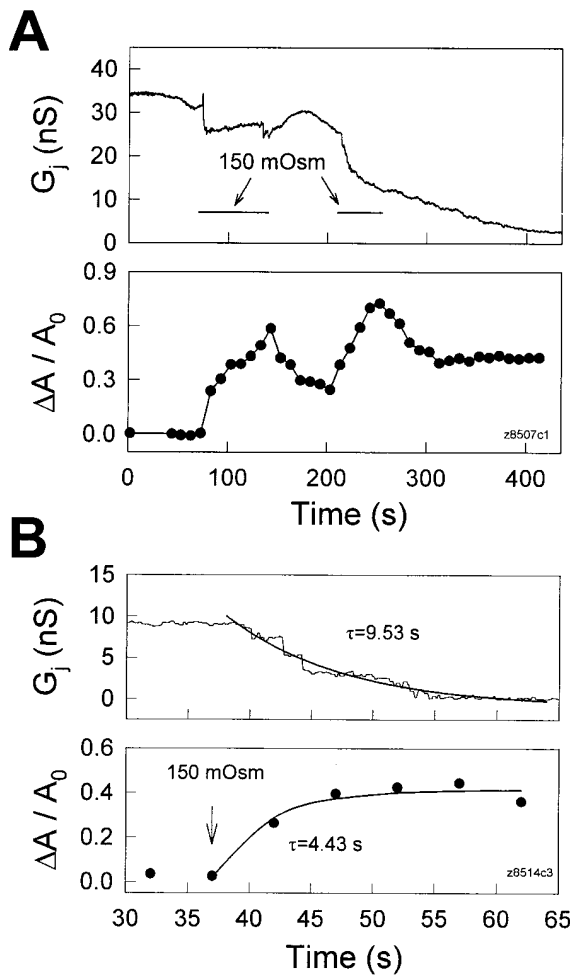


FIGURE 6. (A) Hypo-osmotic solutions induced reversible, concomitant changes in transjunctional conductance and membrane strain. Both cells were held at  $-40$  mV. Repeated applications of 150 mosM solution are indicated by the horizontal bars. (B) The time course of the uncoupling effect caused by hypo-osmotic shock is compared with the increase of membrane strain. The beginning of treatment is indicated by an arrow and continued during the observed period. Thick solid lines represent single exponential fits. Membrane strain appears to have increased before the decrease of  $G_j$ . Pipettes contained  $50 \mu\text{M}$  H-7.

1991). It is possible that membrane tension also alters gating characteristics of supporting cell gap junctions. We show, however, that unlike stretch channels, inner ear gap junctional conductance decreases with membrane stress. Recently, it has been postulated that gap junction channels possess two distinct gating mechanisms, namely, a voltage gating mechanism and a chemical gating mechanism (Bukauskas et al., 1995; Bukauskas and Peracchia, 1997; Bukauskas and Weingart, 1994). Chemical uncoupling agents, such as  $\text{CO}_2$ ,  $\text{H}^+$ , and  $\text{Ca}^{2+}$ , may act on sensor elements from the cytoplasmic side. Supporting cell coupling has been shown to be sensitive to a variety of chemical uncoupling agents (Santos-Sacchi, 1985; 1991), and we now

report that supporting cell coupling is voltage dependent as well. The existence of voltage-dependent gap junctional conductance may account in part for previous reports of temperature-induced depolarization on supporting cell coupling ratios (Santos-Sacchi, 1986). Interestingly, junctional voltage dependence is unaffected by concomitant tension-induced junctional conductance change, possibly indicating that an independent tension gating mechanism may exist.

Gap junctions consist of two aligned transmembrane hemichannels (connexons), one from each cell (Revel et al., 1984; Goodenough et al., 1988; Bennett et al., 1991). Each of these hemichannels is formed by six connexin subunits (Kumar and Gilula, 1996; Perkins et

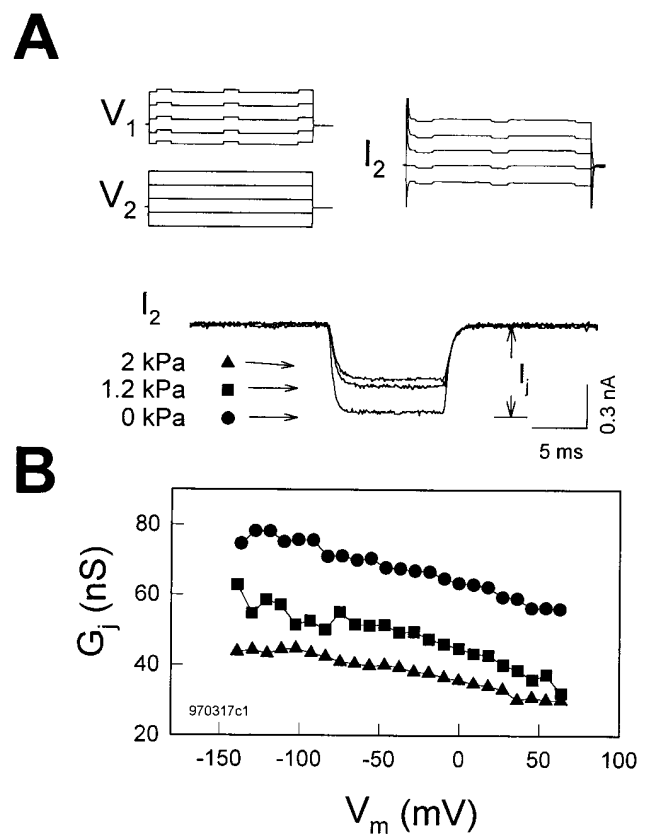


FIGURE 7. Turgor pressure does not affect membrane potential ( $V_m$  or  $V_{i-o}$ ) dependence of gap junctions in Hensen cells. (A) Voltage stimulus protocols for each cell and current trace recorded in cell 2 are plotted (only five traces are shown for clarity). Each cell in a Hensen cell pair was separately voltage clamped at the same holding potential of  $-80$  mV. Voltage steps from  $-140$  to  $70$  mV for  $100$  ms in  $10$ -mV increments were simultaneously delivered into both cells except for  $10$  mV,  $10$ -ms test pulses superimposed on cell 1 only. Transjunctional current ( $I_j$ ) is measured in cell 2. The turgor pressure of cell 1 was directly changed by the patch pipette. Three current traces from cell 2 at different pressures were zeroed and superimposed in the middle. (B) Positive turgor pressure decreased  $G_j$  at all membrane potentials. Note  $G_j$  decrease as the cells were depolarized.  $R_i$  at  $0$  kPa,  $12.5$  M $\Omega$ ; at  $1.2$  kPa,  $12.7$  M $\Omega$ ; at  $2$  kPa,  $12.2$  M $\Omega$ .

al., 1997). Our data indicate that membrane stress acts on inner ear gap junctions in a manner independent of  $\text{Ca}^{2+}$ , pH, and protein kinases. The rapid and reversible nature of the uncoupling also indicates that the mechanism is not due to some sort of mechanical destruction of the channels. While there may be other unknown links between membrane stress and junctional conductance, it is conceivable that tension may gate gap junction channels by a conformational change in connexon structure, possibly causing only the stressed membrane's hemichannel to close.

Gap junction connexins represent a family of homologous proteins that have differing voltage gating characteristics (Harris et al., 1981; Spray et al., 1981; Bennett et al., 1991; Dahl, 1996). Using immunocytochemistry and transmission electron microscopy, Cx26 was found in gap junctions of the rat (Kikuchi et al., 1995) and gerbil (Forge et al., 1997) organ of Corti. More recently, Cx26, Cx30, Cx32, and Cx43 have been localized to supporting cell regions of the rat cochlea (Lautermann et al., 1997). Such diversity of connexins within the organ may provide for a variety of junctional communication characteristics; for example, rectifying junctional conductance. Indeed, in addition to our direct observation that voltage-dependent junctional communication exists in the supporting cells, we have preliminary evidence that junctional rectification occurs. Directional flow of ions mediated by rectified gap junctions may be crucial for normal cochlea homeostasis (see below).

Since the mid 1980's, gap junctional coupling has usually been studied with double voltage clamp. However, input capacitance and resistance reflect the degree of electrical coupling and can be conveniently measured using a single voltage clamp (Santos-Sacchi, 1991; Sato and Santos-Sacchi, 1994; Bigiani and Roper, 1995). Based on a coupled two-cell model (see Fig. 1 B, inset), and assuming that the individual cells have the same input impedance, the following equations are obtained (Bigiani and Roper, 1995),

$$C_{in} = \frac{(2R_m R_j + 2R_m^2 + R_j^2) R_m^2}{(2R_m R_s + R_m^2 + R_s R_j + R_m R_j)^2} C_m, \quad (5)$$

$$R_{in} = \frac{R_s R_j + 2R_s R_m + R_j R_m + R_m^2}{R_j + 2R_m}, \quad (6)$$

where  $R_s$  and  $R_m$  are electrode series resistance and nonjunctional membrane resistance, respectively, and  $C_m$  is single cell capacitance (see Fig. 1 B, inset). Since  $R_m$  is not readily available from recordings, we can solve Eqs. 5 and 6 to remove  $R_m$ .  $R_j$  can be finally expressed:

$$R_j = \left| \frac{C_{in} R_{in}^2 + 4C_m R_s R_{in} - 2C_m R_s^2 - 2C_m R_{in}^2}{\sqrt{2C_m^2 R_s R_{in} + C_{in} C_m R_{in}^2 - C_m^2 R_s^2 - C_m^2 R_{in}^2}} \right|. \quad (7)$$

$C_{in}$ ,  $R_{in}$ , and  $R_s$  are readily obtained from recordings. Fig. 8 illustrates the measurement of these parameters during an uncoupling event, and the bottom panel shows the estimated  $G_j$  based on those data. Changes in estimated  $G_j$  mirror pressure-induced changes in  $C_{in}$ . It should be noted that  $R_s$  changes can also produce changes in  $C_{in}$  and  $R_{in}$ . For example, to obtain the observed maximum change in  $C_{in}$ , an order of magnitude increase of  $R_s$  would be required in this case. In our experiments, changes solely in  $R_s$  required to produce a comparable change in  $C_{in}$  were not observed. Series resistance remained constant, being  $7.79 \pm 0.49 \text{ M}\Omega$  ( $n = 7$ ) for cell pairs that were well coupled and  $6.34 \pm 1.13 \text{ M}\Omega$  after those same cells were uncoupled with positive pipette pressure.

Finally, how might the turgor pressure dependence of junctional coupling in the organ of Corti affect coch-

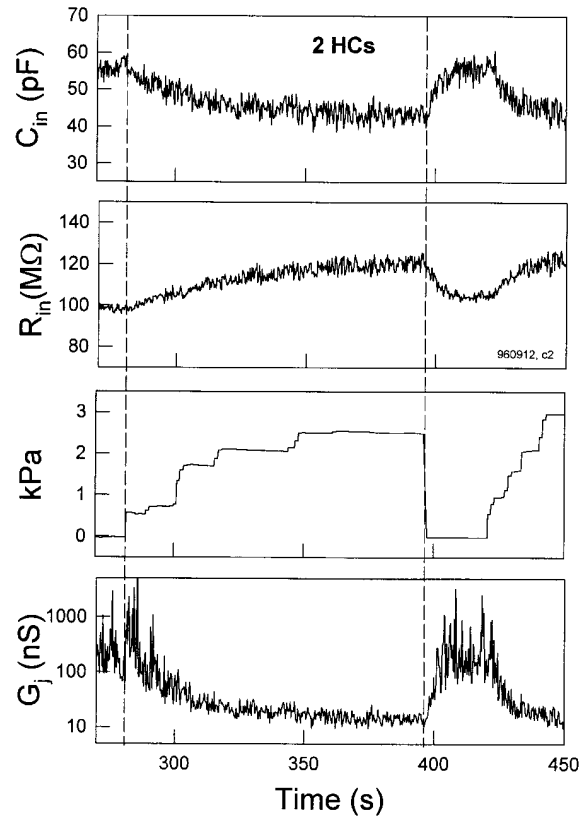


FIGURE 8. Transjunctional conductance is estimated by  $C_{in}$  and  $R_{in}$  in single pipette voltage clamp. (top)  $C_{in}$  decreased and  $R_{in}$  simultaneously increased as turgor pressure increased.  $C_{in}$  and  $R_{in}$  followed changes in pressure.  $R_s$ ,  $8.73 \text{ M}\Omega$ . (bottom)  $G_j$  is estimated from  $C_{in}$  and  $R_{in}$  measurements from the cell pair data based on the coupled two-cell model.  $C_m$  was set as half of  $C_{in}$ ,  $27.5 \text{ pF}$ , at zero applied pressure, and  $R_s$  was  $8.5 \text{ M}\Omega$ . The change in estimated  $G_j$  corresponds well to changes in  $C_{in}$ . The magnitude of  $G_j$  is larger than the largest obtained under double voltage clamp ( $\sim 500 \text{ nS}$ ), and may be due to the fact that cell impedances are not actually identical as required in the model.

lear function? In vivo, the organ of Corti, comprising hair cells and supporting cells, is bathed in two different media, high  $K^+$  endolymph apically and low  $K^+$  perilymph basally. Since the receptor current through hair cells is predominantly carried by  $K^+$ , an accumulation of  $K^+$  within the perilymphatic space along the basolateral region of the hair cells is unavoidable. This would potentially depolarize hair cells with disastrous consequences for both forward and reverse sensory transduction. In the mammal, forward transduction (gating of stereociliar transduction channels) relies on the large driving force present across the hair cell's apical plasma membrane. Voltage gradients across the apical membranes of inner and outer hair cells (i.e., endolymphatic potential minus membrane potential) range from 125 to 150 mV, and drive the  $K^+$ -based receptor currents. Reduction of this gradient (e.g., by membrane depolarization) will reduce the magnitude of receptor potentials and synaptic output. Reverse transduction is a phenomenon that is restricted to the outer hair cell and is believed to provide for the enhanced high frequency selectivity and sensitivity enjoyed by mammals. OHCs, which are additionally mechanically active, possess lateral membrane motors that are driven by voltage (Santos-Sacchi and Dilger, 1988); the cell's mechanical response provides feedback into the basilar membrane, thereby enhancing the stimulus to the primary receptor cells, the inner hair cells (for review see Ruggero and Santos-Sacchi, 1997). Not only will depolarization of the OHC alter the driving force for the mechanical response, but the function relating mechanical response to voltage will be shifted along the voltage axis as well, resulting in an altered gain for the "cochlear amplifier" (Santos-Sacchi et al., 1998). Some mechanisms must prevent such an undesirable scenario. A nutritive and  $K^+$  sinking role for gap junctions

in the avascular organ of Corti has been proposed (Santos-Sacchi, 1985, 1991; Santos-Sacchi and Dallos, 1983). Inner ear supporting cells have been shown to "share" plasmalemmal voltage-dependent conductances due to the high degree of cell coupling (Santos-Sacchi, 1991). The magnitude and stability of their resting potentials is pronounced (close to  $-100$  mV), and likely depends on cell coupling since isolated cell resting input conductance is only  $\sim 1$  nS. At the normal resting potential of this cellular syncytium, an inward rectifier appears continuously activated and may result in  $K^+$  removal from perilymphatic spaces. It should be noted that the large perilymphatic fluid spaces may provide little support in sinking  $K^+$  or directing its movement, since hair cell regions that are likely to experience  $K^+$  elevations are not directly exposed to those spaces. Inner hair cells are closely surrounded by supporting cells, and the region of the OHCs that possesses voltage-dependent conductances (e.g., outward  $K^+$ ) is restricted to the basal pole of the cell (Santos-Sacchi et al., 1997), which is surrounded by a Deiters cell cup. Recently, Kikuchi et al. (1995) provided morphological evidence detailing epithelial and connective tissue gap junctional systems within the cochlea that may complete the mechanism responsible for recycling  $K^+$  from the perilymphatic space near hair cells to the  $K^+$ -rich endolymph via the stria vascularis. The maintenance of normal fluid space architecture within the inner ear requires fine osmotic control; imbalances can lead to serious auditory and vestibular problems (e.g., Meniere's disease). While at present we do not know the normal physiological significance of tension-dependent gap junctional communication, it is likely that fluid balance disorders in the inner ear will affect gap junctional communication, thus compromising sensory function by indirectly modifying hair cell activity.

---

We thank Margaret Mazzucco for technical help.

This work was supported by National Institute on Deafness and Other Communication Disorders grant DC00273 to J. Santos-Sacchi.

*Original version received 12 January 1998 and accepted version received 24 July 1998.*

#### REFERENCES

- Barr, L., W. Berger, and M.M. Dewey. 1968. Electrical transmission at the nexus between smooth muscle cells. *J. Gen. Physiol.* 51:347–368.
- Barr, L., M.M. Dewey, and W. Berger. 1965. Propagation of action potentials and the structure of the nexus in cardiac muscle. *J. Gen. Physiol.* 48:797–823.
- Bennett, M.V.L., L.C. Barrio, T.A. Bargiello, D.C. Spray, E. Hertzberg, and J.C. Saez. 1991. Gap junctions: new tools, new answers, new questions. *Neuron.* 6:305–320.
- Bigiani, A., and S.D. Roper. 1995. Estimation of the junctional resistance between electrically coupled receptor cells in *Necturus* taste buds. *J. Gen. Physiol.* 106:705–725.
- Boulis, N.M., and M. Davis. 1990. Blockade of the spinal excitatory effect of cAMP on the startle reflex by intrathecal administration of the isoquinoline sulfonamide H-8: comparison to the protein kinase C inhibitor H-7. *Brain Res.* 525:198–204.
- Bukauskas, F.F., C. Elfgang, K. Willecke, and R. Weingart. 1995. Biophysical properties of gap junction channels formed by mouse connexin40 in induced pairs of transfected human HeLa cells. *Biophys. J.* 68:2289–2298.
- Bukauskas, F.F., and C. Peracchia. 1997. Two distinct gating mechanisms in gap junction channels:  $CO_2$ -sensitive and voltage-sensitive. *Biophys. J.* 72:2137–2142.
- Bukauskas, F.F., and R. Weingart. 1994. Voltage-dependent gating

- of single gap junction channels in an insect cell line. *Biophys. J.* 67:613–625.
- Dahl, G. 1996. Where are the gates in gap junction channels? *Clin. Exp. Pharmacol. Physiol.* 23:1047–1052.
- Ding, J.P., R.J. Salvi, and F. Sachs. 1991. Stretch-activated ion channels in guinea pig outer hair cells. *Hear. Res.* 56:19–28.
- Forge, A., D. Becker, and W.H. Evans. 1997. Gap junction isoforms in the inner ear of gerbils and guinea pigs. *Br. J. Audiol.* 31:76–77.
- Gale, J.E., and J.F. Ashmore. 1994. Charge displacement induced by rapid stretch in the basolateral membrane of the guinea-pig outer hair cell. *Proc. R. Soc. Lond. B Biol. Sci.* 255:243–249.
- Goodenough, D.A., and N.B. Gilula. 1974. The splitting of hepatocyte gap junctions and zonulae occludentes with hypertonic disaccharides. *J. Cell Biol.* 61:575–590.
- Goodenough, D.A., D.L. Paul, and L. Jesaitis. 1988. Topological distribution of two connexin32 antigenic sites in intact and split rodent hepatocyte gap junctions. *J. Cell Biol.* 107:1817–1824.
- Gulley, R.S., and T.S. Reese. 1976. Intercellular junctions in the reticular lamina of the organ of Corti. *J. Neurocytol.* 5:479–507.
- Hama, K., and K. Saito. 1977. Gap junctions between the supporting cells in some acousticovestibular receptors. *J. Neurocytol.* 6:1–12.
- Harris, A.L., D.C. Spray, and M.V.L. Bennett. 1981. Kinetic properties of a voltage-dependent junctional conductance. *J. Gen. Physiol.* 77:95–117.
- Hoffmann, E.K., and L.O. Simonsen. 1989. Membrane mechanisms in volume and pH regulation in vertebrate cells. *Physiol. Rev.* 69:315–382.
- Huang, G., and J. Santos-Sacchi. 1993. Mapping the distribution of the outer hair cell motility voltage sensor by electrical amputation. *Biophys. J.* 65:2228–2236.
- Iurato, S., K. Franke, L. Luciano, G. Wermber, E. Pannese, and E. Reale. 1976. Intercellular junctions in the organ of Corti as revealed by freeze fracturing. *Acta Otolaryngol.* 82:57–69.
- Iwasa, K.H., M.X. Li, M. Jia, and B. Kachar. 1991. Stretch sensitivity of the lateral wall of the auditory outer hair cell. *Neurosci. Lett.* 133:171–174.
- Iwasa, K.H. 1993. Effect of stress on the membrane capacitance of the auditory outer hair cell. *Biophys. J.* 65:492–498.
- Jahnke, K. 1975. The fine structure of freeze-fractured intercellular junctions in the guinea pig inner ear. *Acta Otolaryngol. Suppl. (Stockh).* 336:1–40.
- Takehata, S., and J. Santos-Sacchi. 1995. Membrane tension directly shifts voltage dependence of outer hair cell motility and associated gating charge. *Biophys. J.* 68:2190–2197.
- Kikuchi, T., R.S. Kimura, D.L. Paul, and J.C. Adams. 1995. Gap junctions in the rat cochlea: immunohistochemical and ultrastructural analysis. *Anat. Embryol.* 191:101–118.
- Kimelberg, H.K., and H. Kettenmann. 1990. Swelling-induced changes in electrophysiological properties of cultured astrocytes and oligodendrocytes. I. Effects on membrane potentials, input impedance and cell–cell coupling. *Brain Res.* 529:255–261.
- Kumar, N.M. and N.B. Gilula. 1996. The gap junction communication channel. *Cell.* 84:381–388.
- Lautermann, J., W.-J.F. ten Cate, K. Jahnke, P. Altenhoff, O. Traub, and E. Winterhager. 1997. Expression pattern of different gap-junction connexins in the rat cochlea. 34th Workshop on Inner Ear Biology. Rosa Marina, Italy. pp. 59. (Abstr.).
- Loewenstein, W.R., M. Nakas, and S.J. Socolar. 1967. Junctional membrane uncoupling: permeability transformations at a cell membrane junction. *J. Gen. Physiol.* 50:1865–1891.
- Ngezahayo, A., and H.A. Kolb. 1990. Gap junctional permeability is affected by cell volume changes and modulates volume regulation. *FEBS Lett.* 276:6–8.
- Perkins, G., D. Goodenough, and G. Sosinsky. 1997. Three-dimensional structure of the gap junction connexon. *Biophys. J.* 72:533–544.
- Revel, J.-P., B.J. Nicholson, and S.B. Yancey. 1984. Molecular organization of gap junctions. *Fed. Proc.* 43:2672–2677.
- Ruggero, M.A., and J. Santos-Sacchi. 1997. Cochlear mechanics and biophysics. In *Handbook of Acoustics*. M.J. Croker, editor. John Wiley & Sons Inc., New York. 1357–1369.
- Santos-Sacchi, J. 1985. The effects of cytoplasmic acidification upon electrical coupling in the organ of Corti. *Hear. Res.* 19:207–215.
- Santos-Sacchi, J. 1986. The temperature dependence of electrical coupling in the organ of Corti. *Hear. Res.* 21:205–211.
- Santos-Sacchi, J. 1991. Isolated supporting cells from the organ of Corti: some whole cell electrical characteristics and estimates of gap junction conductance. *Hear. Res.* 52:89–98.
- Santos-Sacchi, J., and P. Dallos. 1983. Intercellular communication in the supporting cells of the organ of Corti. *Hear. Res.* 9:317–326.
- Santos-Sacchi, J., and J.P. Dilger. 1988. Whole cell currents and mechanical responses of isolated outer hair cells. *Hear. Res.* 35:143–150.
- Santos-Sacchi, J., G.J. Huang, and M. Wu. 1997. Mapping the distribution of outer hair cell voltage-dependent conductances by electrical amputation. *Biophys. J.* 73:1424–1429.
- Santos-Sacchi, J., S. Takehata, and S. Takahashi. 1998. The outer hair cell membrane potential directly affects the voltage dependence of motility-related gating charge. *J. Physiol. (Camb.)* 510:225–235.
- Sato, Y., and J. Santos-Sacchi. 1994. Cell coupling in the supporting cells of Corti's organ: sensitivity to intracellular H<sup>+</sup> and Ca<sup>++</sup>. *Hear. Res.* 80:21–24.
- Spray, D.C., A.L. Harris, and M.V.L. Bennett. 1981. Equilibrium properties of a voltage-dependent junctional conductance. *J. Gen. Physiol.* 77:77–93.
- Suzuki, M., K. Kawahara, A. Ogawa, T. Morita, Y. Kawaguchi, S. Kurihara, and O. Sakai. 1990. [Ca<sup>2+</sup>]<sub>i</sub> rises via G protein during regulatory volume decrease in rabbit proximal tubule cells. *Am. J. Physiol.* 258:F690–F696.
- Yang, X.C., and F. Sachs. 1989. Block of stretch-activated ion channels in *Xenopus* oocyte by gadolinium and calcium ions. *Science.* 243:1068–1070.